Available online at www.sciencedirect.com
SCIENCE DIRECT®
Physica A 367 (2006) 595–612
PHYSICA A
www.elsevier.com/locate/physa

Dynamics of three-state excitable units on Poisson vs. power-law random networks

Anne-Ruxandra Carvunis[a], Matthieu Latapy[b,*], Annick Lesne[c,d], Clémence Magnien[a], Laurent Pezard[e,f]

[a]*Centre de Recherche en Épistémologie Appliquée (CREA), CNRS—École Polytechnique, 1 rue Descartes, F-75005 Paris, France*
[b]*Laboratoire d'Informatique Algorithmique: Fondements et Applications (LIAFA), CNRS—Université Denis Diderot (Paris 7), 2 place Jussieu, F-75251 Paris Cedex 05, France*
[c]*Laboratoire de Physique Théorique de la Matière Condensée (LPTMC), Université Pierre et Marie Curie (Paris 6), 4 place Jussieu, F-75252 Paris Cedex 05, France*
[d]*Institut des Hautes Études Scientifiques, Le Bois-Marie, 35 route de Chartres, 91440, Bures-sur-Yvette, France*
[e]*Laboratoire de Neurosciences Cognitives & Imagerie Cérébrale (LENA), CNRS UPR 640, 47 Bd de l'Hôpital, F-75651 Paris Cedex 13, France*
[f]*Institut de Psychologie, Université René Descartes (Paris 5), 71 Bd Ed. Vaillant, F-92774 Boulogne-Billancourt Cedex, France*

Received 28 September 2005; received in revised form 1 December 2005
Available online 30 January 2006

Abstract

The influence of the network topology on the dynamics of systems of coupled excitable units is studied numerically and demonstrates a lower dynamical variability for power-law networks than for Poisson ones. This effect which reflects a robust collective excitable behavior is however lower than that observed for diffusion processes or network robustness. Instead, the presence (and number) of triangles and larger loops in the networks appears as a parameter with strong influence on the considered dynamics.

Keywords: Complex networks; Excitable dynamics; 3-State cellular automata; Topology

1. Introduction

It has been known for only a few years that most real-world networks (like for instance the internet, social networks, biological networks, and presumably neural networks) have common topological properties, which shows that they are very different from both regular and random networks. In particular, their degree distributions, i.e., for each integer k the fraction p_k of nodes with exactly k links, are very heterogeneous. See [1–5] for experimental evidence based on network reconstruction from extensive data, and [6–11] for theoretical surveys. Quite often, this qualitative heterogeneity can be turned into a quantitative feature: the degree distribution exhibits a power-law decay $p_k \sim k^{-\alpha}$ with exponent α between 2 and 3.5. This is in sharp

*Corresponding author. Tel.: +33 1 44276845; fax: +33 1 44276849.
E-mail address: latapy@liafa.jussieu.fr (M. Latapy).

0378-4371/$ - see front matter © 2006 Elsevier B.V. All rights reserved.
doi:10.1016/j.physa.2005.12.056

contrast with regular lattices (having a constant degree, i.e., single-valued distributions) and random networks (exhibiting Poisson degree distributions) [12,13]. Since then, much work has been done to understand the impact of this property on various phenomena of interest, for instance diffusion phenomena [14–17] and robustness of networks [18–23]. All these studies conclude that there is a strong influence of the network's degree distribution on its behavior: power-law networks are more prone to infections, more vulnerable to targeted attacks, and less sensitive to random failure.

Comparatively very few works have tackled the influence of network topology on the dynamics of units located at the network nodes and coupled along the network links. As a matter of fact, dynamics of coupled units have been mostly studied on regular topologies (and then termed "coupled map lattices"): units are placed on lattices and are coupled either with their neighbors (local coupling) or with all the other units (global coupling) [24]. But the far-from-regular topology of real interaction networks, in particular their heterogeneous degree distribution, strongly suggest these studies' extension to power-law networks [9]. The challenge, for instance in the context of biological networks, e.g. neural networks, is to understand the ways of regulation, optimization, adaptation and control of their dynamics.

In this spirit, we investigated the influence of the topology on the dynamics of a system of very simple excitable units, modeled as a 3-state deterministic automaton. The present contribution thus stands at the crossroads between complex network studies and cellular automata [25–28] and as such, it relies on systematic numerical experiments. Among the possible determinant topological features, we here focused on the one which has been proved to be central in many contexts, namely the degree distribution.

We chose on purpose a minimal dynamic model, to better evidence the role of network topology, with no side effects due to some peculiar detail of the model. Moreover, in order to focus on differences in the dynamics caused by different topological features, the dynamics' rules will remain constant for all the simulations. In such a setting, the complexity originates from the interplay between *global statistical* features of the network (mainly its degree distribution), *local deterministic* updating rules, and *initial conditions*. In consequence the following alternatives are central in our analysis, and will be detailed and discussed all along the exposure: Poisson vs. power-law degree distributions, microscopic vs. macroscopic features, transients vs. asymptotic regimes, typical vs. special instances for the networks and for the initial states.

Similar studies have already been conducted with 2-state units, with two different classes of models for the dynamics: either 2-state cellular automata [29,30], or random Boolean networks [31,32]. In the first class, the state of a node at time $t+1$ is 1 if a sufficiently large number of its neighbors are in state 1 at time t, and 0 otherwise. In the second class, the updating rule is not built on a criterion involving the neighborhood state, but chosen at random (for each node) among all the possible rule tables mappingg each configuration of the node neighborhood to the node output state; a rationale for using such a fully random choice is to account for the presence of both excitatory and inhibitory connections [33,34]. Let us also mention a recent seminal study addressing the same issue of the influence of network topology in the context of evolutionary dynamics on networks modeling population structure [35].

Although a 2-state model has proved to be relevant for modeling associative memory in neural networks [36], it is not sufficient to model typical excitable dynamics, mainly the refractory phase and associated delay in the reactivation. On the contrary, it has been acknowledged for many years that 3-state models are paradigmatic examples of excitable units, see for instance [37–39]. Among the very few papers investigating the influence of the neural network topology on its dynamics, we may cite a study considering sparse networks [40]. More recently, [41] has addressed this question with a model of epileptic seizure as a topologically-induced dynamic transition. But this work relies on a topology which lacks realism, namely an alternative between regular one-dimensional and small-world networks [29].

Experimental investigations of the exact network topology are out of reach at the neural level. At an upper level, evidence for heterogeneity in the degree distribution has been obtained for the network connecting cortical areas in mammalian brains [42]; the authors suggest among other functional implications that such heterogeneous structure and associated degree distribution reflected on cortical activation patterns. This is also discussed in Ref. [43], which motivates further the issues addressed on theoretical grounds in the present paper.

The presentation is articulated as follows. We define our model, notations and investigated properties in Section 2; we also give the details and rationale for the methodological choices involved in the simulations.

We present in Section 3 our first observations on the model. This provides guidelines for a more detailed and systematic numerical exploration, namely a comparative study, for various network topologies, of the influence of initial state (Section 4), the convergence time (Section 5) and the period (Section 6). Section 7 summarizes our results in terms of the influence of topology on the dynamics and presents directions for further research.

2. Preliminaries

Let us first define our dynamic model, namely a deterministic 3-state cellular automaton, and contrast it with two seemingly close models of epidemic spreading, the so-called SIS and SIR models. Concerning investigated properties, we distinguish between microscopic features, at the level of phase space trajectories, and macroscopic order parameters. We will also discuss this below. Finally, we will detail methodological issues.

2.1. The model

Any model accounting for the dynamic behavior of coupled units is defined by two basic ingredients: the network G of coupling interactions and the individual dynamics. The network is described as a pair $G = (V, E)$ where V is the set of units, identified with the nodes of the network, and $E \subseteq V \times V$ is the set of links mediating their interactions. We here considered undirected links, making no distinction between $(u, v) \in E$ and $(v, u) \in E$. The two main parameters are the number N of nodes and the number M of links. The network topology is *locally* characterized by the *neighborhood* $V(v) = \{u \in V, (u, v) \in E\}$ of each node $v \in V$. The number of nodes in $V(v)$, i.e., the number of nodes directly connected to v, is called the *degree of* v. The associated *global*, *statistical* feature is the *degree distribution* $(p_k)_{k \geqslant 0}$ giving for each integer k the fraction p_k of nodes of degree k.

The response of an excitable element (for instance a neuron, a heart cell or certain artificial devices) to a finite stimulus begins with a non-linear burst of activity: the *excited stage*. It is followed by a decrease of the activity below its reference level, during which the element is insensitive to stimuli, hence the name *refractory stage* for this phase. The element then returns to its stable reference state, and remains in this *quiescent state* until it experiences another stimulus. The remarkable fact about real excitable units is that the duration, shape and amplitude of the stimulated dynamic sequence is almost insensitive to the stimulus, provided it is strong enough. This all-or-none, invariant feature leads to the description of the excitable behavior by a deterministic, discrete time and symbolic dynamics. Each node $v \in V$ can be in three different states: *quiescent* (q), *excited* (e) and *refractory* (r). We denote by $s_t(v) \in S = \{q, e, r\}$ the state of v at discrete time t.

In a network, the stimulus experienced by the unit v comes from the excitable units coupled to v, namely $u \in V(v)$. We here consider the case when the excitation of one neighbor $u \in V(v)$ is enough to excite v. The behavior of v will be the same if a larger number of its neighbors are simultaneously excited. Such all-or-none output obviously smoothes out fluctuations in the inputs received by v as well as superimposed noise, further supporting the consideration of a deterministic dynamic framework. Accordingly, the evolution of the system is achieved through a synchronous updating at discrete times (with a constant time step $\Delta t = 1$) according to the following rules:

- a quiescent node becomes excited if at least one of its neighbors was excited at the previous step: if $s_t(v) = q$ and there exists $u \in V(v)$ such that $s_t(u) = e$, then $s_{t+1}(v) = e$; otherwise $s_{t+1}(v) = s_t(v)$,
- an excited node becomes refractory at the next step: if $s_t(v) = e$ then $s_{t+1}(v) = r$,
- a refractory node becomes quiescent at the next step: if $s_t(v) = r$ then $s_{t+1}(v) = q$.

Note that these dynamic rules are applicable to any topology. This model satisfies the "quiescent condition" [25]: the state where all nodes are quiescent is an equilibrium state (and is the only one). Since it is a deterministic dynamics, we can easily compute any state $s_{t'}(V)$ for $t' \geqslant t$ if we know $s_t(V)$ (and of course G). An instance of the model is then entirely defined by a pair $(G, s_0(V))$ where G is a network, V its set of nodes and

$s_0(V)$ its initial state. The dynamics' rules prevent self-inputs, since only excited nodes influence quiescent states, hence a node never influences itself; in consequence, $(v,v)\notin E$ by convention.

The choice of a threshold equal to 1 implies that excitation of a node is transmitted to all its quiescent neighbors: the neighborhood size will thus presumably act as an amplifier (around hubs, i.e., nodes of high degree) or a suppressor (around nodes of low degree, e.g. in a linear chain). Excitation locally propagates into quiescent regions, followed by an edge of refractory states, then by quiescent states. The existence of refractory states prevents back propagation: excitation transmitted from v to u at time t cannot be transmitted back to v at time $t+1$. Re-entrance of excitation in v might occur only if there exists closed paths (named *cycles*) allowing to bypass the refractory line. These qualitative properties, associated with a local excitability threshold equal to 1, hint at an influence of the topology on the collective dynamics (beyond the mere global threshold effect that would arise with values larger than 1 for the local threshold). This supports our choice of this model as presumably the best-suited to the issue addressed here.

2.2. Comparison with SIS/SIR models

Two models seemingly very close to the above one, namely SIS and SIR, have been widely studied in the literature, in particular, in what concerns the influence of the network topology (e.g. the difference in behavior on Poisson and power-law networks).

In the SIS model, see for instance [44,45], the unit is either *susceptible* or *infected*; its state thus belongs to $S=\{s,i\}$ and evolves according to the following dynamic rules:

- if $s_t(v)=s$ and there exists $u\in V(v)$ such that $s_t(u)=i$, then $s_{t+1}(v)=i$; otherwise $s_{t+1}(v)=s_t(v)$,
- if $s_t(v)=i$, then $s_{t+1}(v)=s$.

The main difference with our model lies in the absence of a delay in the recovery (no refractory state). Backward propagation is then possible and it has crucial consequences on the results as we shall see in the following.

In the SIR model [44,46,47], the state space is $S=\{s,i,r\}$, for *susceptible*, *infected* and *removed*, respectively. These names reflect the updating rules:

- if $s_t(v)=s$ and there exists $u\in V(v)$ such that $s_t(u)=i$, then $s_{t+1}(v)=i$,
- if $s_t(v)=i$ then $s_{t+1}(v)=r$,
- in the other cases $s_{t+1}(v)=s_t(v)$.

Therefore, a node reaching the *removed* state does not evolve anymore and has no influence on its neighbors; it might be ignored. In consequence, infection dies out in a finite network or runs away from its source in an infinite one. This model thus captures only propagating front waves of infection starting from the initially infected nodes.

Let us finally underline that, in our model, investigating the influence of the local excitability threshold value (fixed to 1 in the present study) would have been very close to studies conducted on SIR/SIS models [14,15]. These studies evidence a critical value (quite analogous to a percolation threshold) above which infection or equivalently excitation transmission is so hampered that it fades away to 0 (recall that it is short-lived at a given site). This issue, mentioned in our perspectives, is nevertheless out of our present focus.

2.3. Microscopic observables

Given an instance $(G,s_0(V))$ of our model, its dynamics is nothing but a trajectory in the phase space S^N containing the 3^N possible configurations of the N node states (this is the viewpoint of dynamical system theory). The phase space S^N being finite, any trajectory $[s_t(V)]_{t\geqslant 0}$ is eventually periodic. We define the *period* $p(G,s_0(V))$ of the system as the smallest integer $p>0$ such that $s_t(V)=s_{t+p}(V)$ for a time t. Since the dynamics is discrete in time, trajectories originating from different initial conditions could merge. In particular, before reaching its asymptotic periodic regime, a trajectory will in general exhibit a transient, non-periodic regime,

whose duration will be called the (microscopic) *convergence time*. More precisely, we define the convergence time $c(G, s_0(V))$ of the system as the smallest integer t such that $s_t(V) = s_{t+p}(V)$ for an integer p.

2.4. Macroscopic observables

Given the state $s_t(V)$ of the system at a given moment t, one may also observe the *macroscopic* state $S_t(V) = (f_t(q), f_t(e), f_t(r))$ where $f_t(q), f_t(e)$, and $f_t(r)$ denote the fractions of quiescent, excited, and refractory nodes at time t, respectively. This is a viewpoint in the spirit of statistical mechanics, and the fractions are termed the "order parameters" of the system in this context. These global statistics, providing macroscopic summary of the system state, will be of great importance in the following. At this macroscopic level, the dynamics of an instance of our model is a trajectory in the macroscopic state space $[0, 1]^3$. This trajectory might have a period, denoted by $P(G, s_0(V))$ but we cannot define it using the first time the same macroscopic state is reached twice. Indeed, this does not mean that it will be reached again, since it may stand for different microscopic states. We therefore define it as the smallest integer $p > 0$ such that there exists a time t such that for all integer i: $S_t(V) = S_{t+ip}(V)$. The smallest such t is called the macroscopic convergence time $C(G, s_0(V))$ of the system.

Notice that we always have $C(G, s_0(V)) \leqslant c(G, s_0(V))$ and $P(G, s_0(V)) \leqslant p(G, s_0(V))$. We can even notice that $p(G, s_0(V))$ is a multiple of $P(G, s_0(V))$ and that there may be many instances such that $P(G, s_0(V)) = 1$, whereas the only cases where $p(G, s_0(V)) = 1$ is when there exists a time t at which $s_t(v) = q$ for all $v \in V$, i.e., if the trajectory reaches the unique (microscopic) equilibrium state of the dynamics.

2.5. Random networks

There is a huge variety of networks on which the dynamics may be studied (the updating rules define a consistent evolution whatever may be the underlying topology). We however have specific questions in mind, mainly the impact of the underlying degree distribution on the system behavior. Accordingly, we look for possible differences between the dynamics on *qualitatively* different topologies, spanned by the paradigmatic Poisson and power-law degree distributions. We used the two following models (implementations of these models are available at [48], see also methodological details at the end of the present section).

- The first one is the classical Erdös–Rényi model [12,13], which samples uniformly at random networks among all the ones with a given number N of nodes and a given number M of links by choosing M pairs at random. At the infinite limit, this random network model is equivalent to the model where the network is constructed from a given number N of nodes, each possible link being added with a probability p (independently of the other links).
- The second one is the *configuration* model [49], which samples uniformly at random networks among all the ones with a given number N of nodes and a given degree distribution $(p_k)_{k \geqslant 0}$. One first samples the degree of each node according to the degree distribution, and then links random pairs of nodes as long as they do not have as many links as this degree.

Note that in both models the connections are symmetric: the excitation might propagate both ways. The presence of a refractory step nevertheless prevents from immediate backward propagation, as noticed above.

The Erdös–Rényi model gives networks with Poisson degree distributions, $p_k \sim e^{-\lambda} \lambda^k / k!$; it thus exhibits a typical degree λ (coinciding with the average degree) and an exponential decrease $p_k \sim e^{-k \ln(1/\lambda)}$ for large k values. These networks therefore do not fit the heterogeneous degree distributions met in practice.

To generate more realistic model networks, we shall use the *configuration* model, able to produce networks with power-law degree distributions $p_k \sim k^{-\alpha}$ (also termed "scale-free networks" since a power-law degree distribution does not put forward any characteristic degree value, i.e., there is no typical scale for the degree). Notice that it is *not* the classical Albert–Barabási model [50] often used to generate power-law networks. The configuration model has the advantage of producing networks with any prescribed degree distribution, which is crucial here. The exponent of the law should satisfy $\alpha > 1$ so that the distribution can be normalized to 1. Power-law networks have a high fraction of small-degree nodes, but also a non-negligible number of very-high

degree nodes. In consequence, the statistical average degree $\langle k \rangle$ no longer coincides with any typical degree value. It is besides well-defined only for $\alpha > 2$. It is possible to compute the exact expression of $\langle k \rangle$ as a function of α, but for qualitative discussion, the rough estimate $\langle k \rangle \approx (\alpha - 1)/(\alpha - 2)$ obtained in the continuous approximation for k will be more useful. Average degree is then larger than 3 for $\alpha < 2.5$.

2.6. Random initial states

As there are many ways to choose a network $G = (V, E)$ to define an instance of our model, there are many ways to choose an initial state $s_0(V)$. In order to keep things simple and to focus on the influence of the topology on the dynamics, with the least possible non-topological sources of bias, we used random initial states. This will prove to be sufficient in the following.

More precisely, given three positive numbers p_q, p_e and p_r with $p_q + p_e + p_r = 1$, we sample independently the state of each node, this state being quiescent, excited or refractory with probability p_q, p_e and p_r, respectively. We call an initial state obtained in this way a (p_q, p_e, p_r)-*initial state*. Accordingly, the fractions $[f_0(q), f_0(e), f_0(r)]$ of nodes in each state are random variables. Only their statistical mean are prescribed, respectively equal to (p_q, p_e, p_r), with a fluctuation of order $O(1/\sqrt{N})$ where N is the total number of nodes.

2.7. Mean-field approach

Given the model and its dynamics, analytical studies rely on a mean-field-like approach [30]. Let us sketch its basic principles, features and flaws, motivating our numerical approach.

For any node $v \in V$ and state $\sigma \in S$, let us denote by $c_t(\sigma, v)$ the Boolean function equal to 1 if $s_t(v) = \sigma$ and 0 otherwise. We then have for all v, $\sum_{\sigma \in S} c_t(\sigma, v) = 1$ and for all σ, $f_t(\sigma) = (1/N) \sum_{v \in V} c_t(\sigma, v)$. Denoting $Y()$ the Heaviside function ($Y(x)$ equals 1 if $x \geqslant 0$ and 0 otherwise), the dynamics is described by the three following equations, for all $t \geqslant 0$ and $v \in V$:

$$c_{t+1}(r, v) = c_t(e, v),$$

$$c_{t+1}(e, v) = c_t(q, v) \cdot Y\left[\sum_{u \in V} l(u, v) c_t(e, u) - 1\right],$$

$$c_{t+1}(q, v) = 1 - c_{t+1}(r, v) - c_{t+1}(e, v),$$

where $l(u, v)$ is 1 if the link (u, v) exists and 0 otherwise.

In the mean-field framework, one approximates the average of products $(1/N) \sum_{u \in V} l(u, v) c_t(e, u)$ by the product of averages $(1/N) \sum_{u' \in V} l(u', v)(1/N) \sum_{u \in V} c_t(e, u)$. But $\sum_{u \in V} l(u, v)$ is nothing but the degree k_v of v and $\sum_{u \in V} c_e(t, u)$ can be approximed by $N f_t(e)$. The main equation above then becomes

$$c_{t+1}(e, v) = c_t(q, v) \cdot Y(k_v f_t(e) - 1).$$

At this stage, we can obtain an interesting conclusion concerning our model. Consider an instance $(G, s_0(V))$ with period $p(G, s_0(V)) = 3$. One can easily show (we will provide a proof below) that this implies that no node stays in the same state (including the quiescent one) more than one time step in a row. In the mean-field framework, this requires that $k_v f_t(e) \geqslant 1$ for all $v \in V$, i.e., $k_v \geqslant 1/f_t(e)$: a mean-field approach could be valid only if the average degree is large enough, which will be confirmed by experiments in the following.

We see from the above equations that this mean-field approach has turned the original cellular automata into a coupled map lattice, composed of N units with two variables $[c_t(q), c_t(e)]$ each. Such coupled map lattices do not faithfully account for all the correlations present in the original system. Moreover, to get analytically tractable equations, one has to further reduce the description and work at the level of fractions $f_t(\sigma)$, $\sigma \in S$ (or at best at the level of pair correlation functions describing the joint statistics of the states of a pair of neighbors). Further decoupling approximations are then required to get closed evolution equations. Notwithstanding the questionable validity of the involved approximations, the resulting framework is obviously not a relevant approach to study dynamic properties at the level of trajectories, since it cannot capture notions like period, convergence time, etc. on which this paper focuses. It can neither fully account for

the spatial heterogeneity and correlations. In consequence, the issues addressed in this paper are entirely out of reach in a mean-field approach, motivating our empirical, though rigorous, approach based on numerical simulations.

2.8. Methodology

The networks obtained with the models presented above are not always connected, i.e., there does not exist a path between all pairs of nodes. The dynamics then runs independently on the various connected components, hence what really makes sense is to consider only the largest connected component. The ensuing flaw in comparative studies is the possibly varying size $N_{cc} \leqslant N$ of this connected component. Generating random *connected* networks with prescribed degree distribution is possible but it is a difficult task [51] and it has important drawbacks in our context. Moreover, whenever the average degree is not too low (basically larger than 2), the largest connected component contains most (if not all) nodes [12,49,52]. Finally we decided not to include the connectedness constraint in the generating procedure, but rather to keep a posteriori the largest connected component. This is very classical in complex network studies.

We call a *λ-Poisson network* any network obtained by generating a Poisson network of average degree λ with the Erdös–Rényi model and then keeping only its largest connected component. This restriction slightly modifies the degree distribution, e.g. the probability that a node has degree $k = 0$ now vanishes, which implies that the normalization of the initial Poisson distribution is modified accordingly; in consequence, λ-Poisson networks have an average degree larger than λ, roughly by a factor of $1/(1 - e^{-\lambda})$. If λ is larger than 2, however, the two networks are almost identical (since $p_0 = e^{-\lambda} \ll 1$), and the larger λ the more identical they are. Likewise, we call an *α-power-law network* any network obtained by generating a random network with degree distribution $p_k \sim k^{-\alpha}$ with the configuration model and then keeping only its largest connected component. The largest connected component is small (less than 10% of the network) only for $\alpha > 3.5$ (then $\langle k \rangle < 2$) whereas it almost, if not exactly, coincides with the whole network for $\langle k \rangle > 2$ (i.e., smaller α values). Like in λ-Poisson networks, restriction to the connected component implies that α-power-law networks have an average degree slightly larger than the average degree of the original network. Likewise, their degree distribution may differ significantly from a power law with exponent α at low values of k. But in most cases the connected networks are almost identical to the original ones, and most importantly, their degree heterogeneity, which is the relevant feature in the present study, are comparable. In conclusion, the restriction to the largest connected component has no impact in most practical cases, since the original network is connected whenever the average degree is not too close to 2. In some limited cases, however, it may have an influence on the interpretation of our results, which will then be discussed accordingly.

All the networks considered in the simulations will be λ-Poisson or α-power-law networks, as described above. The parameters of interest, quantifying the network topology, are the average degree in the first case, and the power-law exponent in the second case. To compare these different classes of networks, we shall often express the results on power-law networks in terms of their average degree (empirical average computed in each sample) in addition to their exponent. In numerical studies, in order to minimize sampling and finite-size effects, we shall always consider the empirical average degree, computed in each configuration as an average over all the nodes of the connected component. Parameter ranges considered here will cover the values met in practice, namely λ from 1 to 20 and exponents α from 1.5 to 5. The parameters leading to average degrees close to 2, basically λ between 1 and 2.5 and α larger than 3 generate extremal cases as explained below.[1]

The initial states considered in all the simulations will be random initial states, inducing some variability from one sample to another. Due to the strong coupling between neighboring units and the ensuing collective behavior of the network, it is a priori possible that changing only one node's initial state has significant consequences on the overall dynamics. However, the investigations conducted on this possible sensitivity showed that it does not affect the observables considered in the present paper (convergence time, period and average excitation), thus validating a plain random sampling of the initial state.

[1]The average degree cannot be significantly lower than 2 in a connected component, the worst case being that of trees, where it is equal to $2(N - 1)/N$.

From a probabilistic point of view, network configurations where the average degree k is close to 2 or (p_q, p_e, p_r)-initial states with at least one very low p_σ (with $\sigma \in S = \{e, q, r\}$), are very rare; moreover, the variability is high in these extreme cases. We shall therefore call them *non-typical* cases whereas the other cases will be called *typical* cases. We expect, and our results will confirm this, that the observed behaviors are very robust in typical cases, whereas they are less reproducible, i.e., more sensitive to minute variations of network configuration or initial state, in non-typical cases.

Let us end this section with a few technical points. All the networks considered in the paper have $N = 1000$ nodes. This is large enough to avoid small-size effects (which we checked on larger networks), to capture a representative view of the dynamics and to get a good statistical behavior. For instance, when performing the random initialization with probabilities p_e, p_r and p_q, the associated fluctuations of, say, $f(q)$ is 1% or 2% percents (more precisely, $\delta f(q) \approx \sqrt{p_q(1-p_q)/N}$, i.e., $\delta f(q) \approx 0.015$ for $p_q = \frac{1}{3}$). Moreover, considering larger networks would make some of our experiments computationally intractable.

Our simulations have been performed on networks with average degree up to $\langle k \rangle = 20$: indeed, preliminary tests have shown no significant differences in observable properties between this maximal value and higher values of the average degree. Finally, for all investigated quantities x (the fractions $f(\alpha)$, the convergence time, the period), we chose to visualize the statistical dispersion over a sample by plotting the ensemble average $\bar{x}$, together with this value plus (resp. minus) the average difference Δx^+ (resp. Δx^-) between values larger than $\bar{x}$ (resp. smaller) and $\bar{x}$. The rationale for considering such differences $\Delta x^\pm$, rather than the standard deviation, is to visualize separately the dispersion of x towards larger (resp. smaller) values than the ensemble average $\bar{x}$. Moreover, the interval $[\bar{x} - \Delta x^-, \bar{x} + \Delta x^+]$ gives a better estimate of the typical range of values of x in case of non-Gaussian statistics.

3. Basic properties of the dynamics

We here present some general properties of the dynamics, providing hints and guidelines in devising the systematic numerical studies presented in the following sections.

As already discussed, any trajectory of our model always reaches a periodic regime with period p, whatever the network topology and the initial state. This implies a periodic behavior at the macroscopic level too. Moreover, the relations $f_{t+1}(r) = f_t(e)$ and $f_t(q) = 1 - f_t(e) - f_t(r)$ imply that if one fraction $f_t(\sigma)$ is periodic, the two other are also periodic with the same period, denoted by P.

The series of fractions $(f_t(\sigma))_{t \geqslant 0}$ for each $\sigma \in S = \{q, e, r\}$ therefore, are all periodic with the same period P. We insist however on the fact that there is no other obvious relation (with or without delay) between these fractions, and that the microscopic period p cannot be deduced from them: we can only state that p is an integral multiple of the macroscopic period P. The full dynamics in the phase space S^N deeply depends on the underlying topology (and possibly on its initial state). We elaborate further on this fact below, first by showing what *can* (and cannot) occur with our model, then by examining representative instances, and finally by studying average and extremal behaviors in typical and non-typical cases.

3.1. Possible and impossible behaviors

From the very definition of the model, one can easily notice that the smallest non-trivial period is $p = 3$ (whereas $p = 2$ is possible in the SIS model, for instance). It is in particular observed in any elementary pattern of 3 nodes connected into a triangle and initially in the state (e, q, r), then evolving by a mere circular permutation of the individual states (namely (r, e, q), then (q, r, e) and back to (e, q, r)). A remarkable fact concerning such a triangle is that its periodic behavior is preserved upon embedding into a larger network, whatever its topology and initial state: when the initial state contains such a triangle, the period p of any trajectory will necessarily be an integral multiple of 3, and excitation never dies out. The only state in which the period is 1 is the one where all the nodes are in the quiescent state. This state can be reached from many initial states (with the above-mentioned necessary condition that they do not contain a triangle in the state (e, q, r)). Therefore, we expect that excitation dies out less frequently in power-law networks, due to the higher

probability of finding triangles (e,q,r) in the initial state (there are significantly more triangles in power-law networks than in Poisson ones [7]).

There is clearly no upper limit for the microscopic period p. Consider for instance a ring of n links: $G=(V,E)$ with $V=\{0,...,n-1\}$ and $E=\{(i,i+1 \bmod n),\ i\in V\}$, and an initial state in which all nodes are quiescent except two adjacent ones, one in excited state and the other in refractory state, i.e., $s_0(v)=q$ for all $v>1$, $s_0(0)=r$ and $s_0(1)=e$. At each time step, the excitation and the following refractory state jump one node forward, hence the period is $p(G,s_0(V))=n$.

At the macroscopic level too, the smallest non-trivial period cannot be lower than $P=3$. But many microscopic evolutions may underly a macroscopic period of 1. They include of course the equilibrium state ($s_t(v)=q$ for any time t and any node $v\in V$) but also many non-equilibrium regimes, as illustrated by the above ring configuration for which $f_t(q)=(n-2)/n$, $f_t(e)=f_t(r)=1/n$ all along the time, and thus $P=1$.

Here again we can build examples with arbitrarily large period P. Consider for instance a network made of two linear branches $(u_1,\ldots,u_{n-1})$ and $(v_1,\ldots,v_{n-1})$, stemming from the same node u_0 and joining in a node u_n, then closed with an additional link from u_n to u_0. Starting from an initial state in which $s_0(u_0)=e$, $s_0(u_n)=r$, and all other nodes are in the quiescent state leads to a periodic trajectory of macroscopic period $P=n+1$ (which happens to be equal to the microscopic period p in this particular case). Another meaningful example is provided by a "decorated ring": a network composed of a ring of n links and an additional node connected to one node on the ring (a "dangling end", see below): $G=(V,E)$ with $V=\{0,...,n\}$ and $E=\{(i,i+1 \bmod n),\ 0\leqslant i\leqslant n-2\}\cup\{(n-1,0)\}\cup\{(0,n)\}$. Then, again consider an initial state where all the nodes are quiescent except two adjacent ones, one in the excited state and the other in the refractory state, i.e., $s_0(v)=q$ for all $v>1$, $s_0(0)=r$ and $s_0(1)=e$. Then the macroscopic period is $P(G,s_0(V))=n$ (here equal to the microscopic period). Actually, the presence of the dangling end affects only the macroscopic period (it would be $P'=1$ in a plain ring, whereas the microscopic period would still be $p'=n$).

The same kind of remarks can be done concerning the convergence time. One can for instance consider a chain of length n: $G=(V,E)$ with $V=\{0,...,n\}$ and $E=\{(i,i+1),\ 0\leqslant i<n\}$ with all nodes initially in the quiescent state, except node 0 in excited state: $s_0(v)=q$ for all $v>0$ and $s_0(0)=e$. Then the system will reach the equilibrium state where all the nodes are quiescent (with period 1) only after $n+2$ time steps. This example also stands for macroscopic convergence time, which is equal to the microscopic one in this case.

These examples show that both period and convergence time are non-trivial features of the model and deserve more attention. Moreover, they underline the importance of carefully distinguishing between the two levels, termed microscopic and macroscopic, at which one may observe the model.

Before entering in the first details of our numerical experiments, let us make a last remark: if a system is in a non-trivial periodic regime then all its nodes contribute to the dynamics in the sense that no node stays in the same state forever. This is obvious for all states but the quiescent one. Suppose therefore there is a node remaining forever in the quiescent state. This implies that none of its neighbors passes through the excited state (else it would force it to change its state). Hence after at most one step (some of the node's neighbors may be in the state r), all its neighbors are in the q-state. By repeating this reasoning, we see that all nodes must ultimately be in the quiescent state, which is in contradiction with our hypothesis. This proves the claim. Notice however that the state of some nodes may change only once per period and that the period can be arbitrarily large, as explained above. If the period is 3 (its minimal non-trivial value), however, these remarks imply that no node stays in the same state more than one time step in a row.

The discussion above gave intuition on what *can* happen in the dynamics we observe. We gave some instances which show that some particular behaviors are *possible*, which will be useful to understand the experiments below. These behaviors may however be very rare and may never occur in typical instances following from a random sampling. To explore this, we present now numerical experiments aimed at observing what happens in typical and special cases.

3.2. Representative examples of the dynamics

We shall here observe and discuss the typical behaviors obtained on a given network with given initial states. Since the behaviors discussed here are the same for Poisson and power-law networks, we shall only present the Poisson cases.

We plot in Fig. 1 the evolution of $f_t(\sigma)$ for each $\alpha \in S = \{q, e, r\}$, in two different cases: a typical Poisson network (large value $\lambda = 10$, Fig. 1a) and a non-typical one (small value $\lambda = 1$, Fig. 1b), both with typical initial states.

The typical case (Fig. 1a) is representative of what is observed on most such instances: the system reaches a macroscopic periodic regime of period $P = 3$ after a short macroscopic convergence time (generally $C \leqslant 4$ time steps). In such cases, we generally observe that both the period and the convergence time are equal at the microscopic and macroscopic levels, i.e., $p = P$ and $c = C$ (which is by no means neither obvious nor necessary, as illustrated in the previous subsection).

For non-typical Poisson networks (Fig. 1b), a significant macroscopic convergence time (larger than 40 time steps in the example) is observed, with high variability. Recall that it provides a lower bound for the microscopic convergence time ($c \geqslant C$), which therefore is large too. Likewise, the period (which is too large to be observed on the figure) can be large and has an important variability.

These observations are only a qualitative preliminary step, leading to the quantitative investigations presented in the following sections, which supports their representativity.

3.3. Average and extremal behaviors

To enlighten the macroscopic behavior we may *expect*, we sample 1000 networks with the same average degree and macroscopic initial states. The obtained ensemble average, minimum and maximum values of the fraction of quiescent nodes at each time step are plotted in Fig. 2 (the fractions concerning other states are observed to behave similarly). The fact that the ensemble average and extremal behaviors in typical cases (Fig. 2a) is very similar to the behavior of any individual sample (Fig. 1b) confirms that both the convergence time and the period are very robust, with respect to the microscopic details of both the underlying topology and the initial state. In other words, in typical cases, the average degree and the initial fractions of nodes in

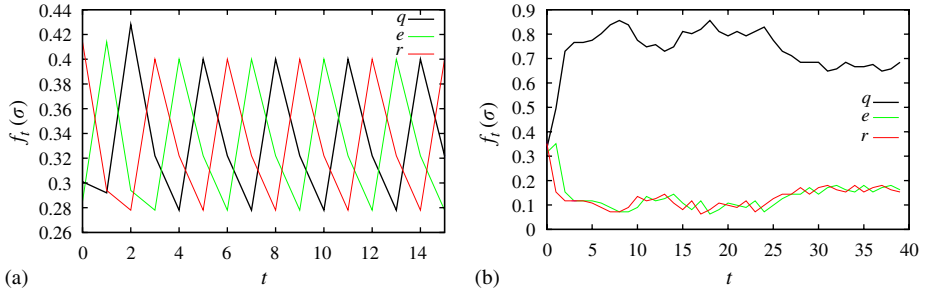

Fig. 1. Examples of evolutions observed on the fractions $f_t(\sigma)$ with $\sigma \in S = \{q, e, r\}$ (i.e., at the macroscopic level) for λ-Poisson networks with typical $(0.3, 0.3, 0.4)$-initial states. (a) For a (typical) 10-Poisson network and (b) for a (non-typical) 1-Poisson network.

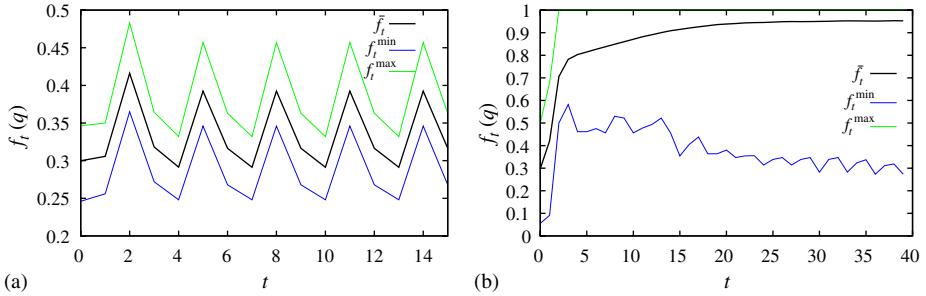

Fig. 2. Ensemble average, minimal and maximal values (resp. $\bar{f}_t$, $f_t^{\min}$ and $f_t^{\max}$) for the fraction $f_t(q)$ of quiescent nodes in λ-Poisson networks with typical $(0.3, 0.3, 0.4)$-initial states. (a) Over 1000 instances of 10-Poisson networks and (b) over 1000 instances of 1-Poisson networks.

each state prescribe both the period and the convergence time. Otherwise, averaging over 1000 network instances would smooth out the oscillations and the ensemble average would be constant.

This latter behavior is actually that observed for non-typical Poisson networks (still with typical initial states), where the ensemble average fraction of quiescent nodes collapses to a constant (Fig. 2b). In fact, such systems can reach the state where *all* the nodes are quiescent $f_t(q) = 1$, thus corresponding to the microscopic equilibrium state and not only to a macroscopic stationary regime. This extinction happens quite often, which noticeably increases the ensemble average value $\bar{f}_t(q)$. This point is discussed further in the next section.

4. Influence of initial states

In the previous section we compared basic macroscopic properties of the dynamics on typical vs. non-typical networks while the initial states were always typical ones: concerning these coarse dynamic features, Poisson and power-law networks behave similarly. We now explore the influence of initial states, either typical or non-typical, on the dynamics observed at the macroscopic level.

Let (α, β, γ) denote a permutation of (q, e, r). To quantify the influence of the initial state (characterized by any two fractions $f_0(\beta)$ and $f_0(\gamma)$), we observed, in the periodic regime, the mean (i.e., time-averaged over a period) and extremal fractions of nodes in state α as a function of $f_0(\beta)$, for a given fraction $f_0(\gamma)$. Numerical experiments were conducted for a wide range of initial fractions and general classes of behaviors were observed. These representative situations are illustrated here using a constant initial fraction of refractory nodes $f_0(r) = 0.3$ ($\gamma = r$) and an initial fraction of excited nodes ($\beta = e$) varying from 0 to $1 - f_0(r) = 0.7$. The results are plotted in Fig. 3 for both typical and non-typical Poisson and power-law networks.

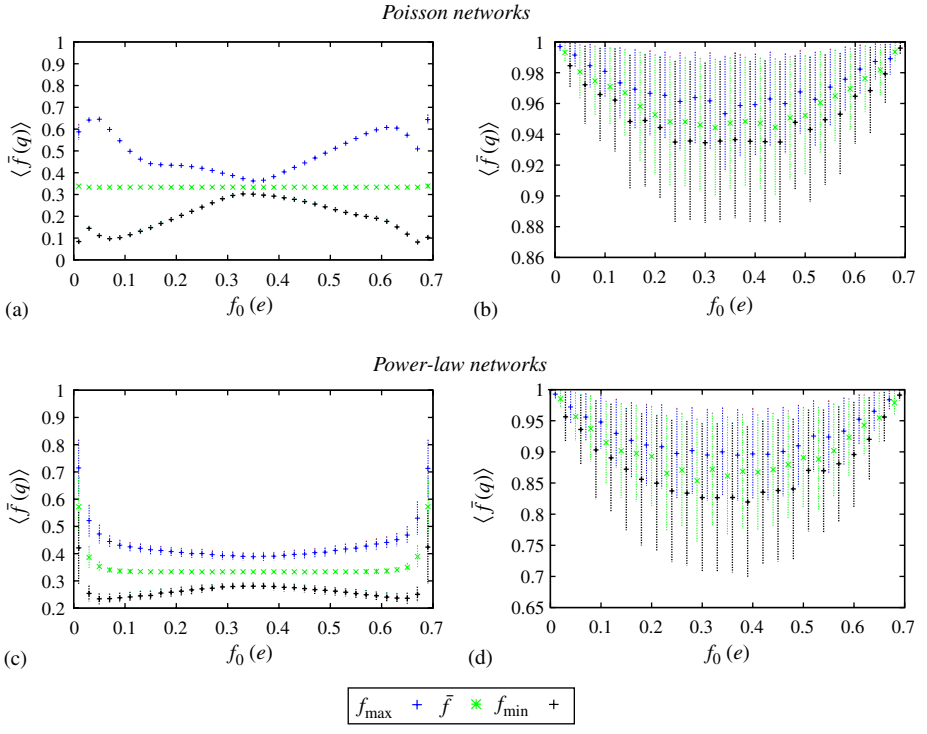

Fig. 3. Ensemble average of the mean fraction (time average over a period) of quiescent nodes $\langle \bar{f}_t(q) \rangle$ and its statistical dispersion in the asymptotic periodic regime as a function of the initial fraction $f_0(e)$ of excited nodes, with $(1 - 0.3 - f_0(e), f_0(e), 0.3)$-initial states. (a) For 10-Poisson networks, (b) for 1-Poisson networks, (c) for 2.5-power-law networks and (d) for 3.5-power-law networks. For each value of $f_0(e)$, we plot the ensemble average over a set of 1000 instances of the time-averaged value of $f_t(q)$; its statistical, possibly asymmetric, dispersion is visualized by plotting the average plus (resp. minus) the average difference between it and values larger (resp. smaller) than it. See the end of Section 2.8 for details on our notations.

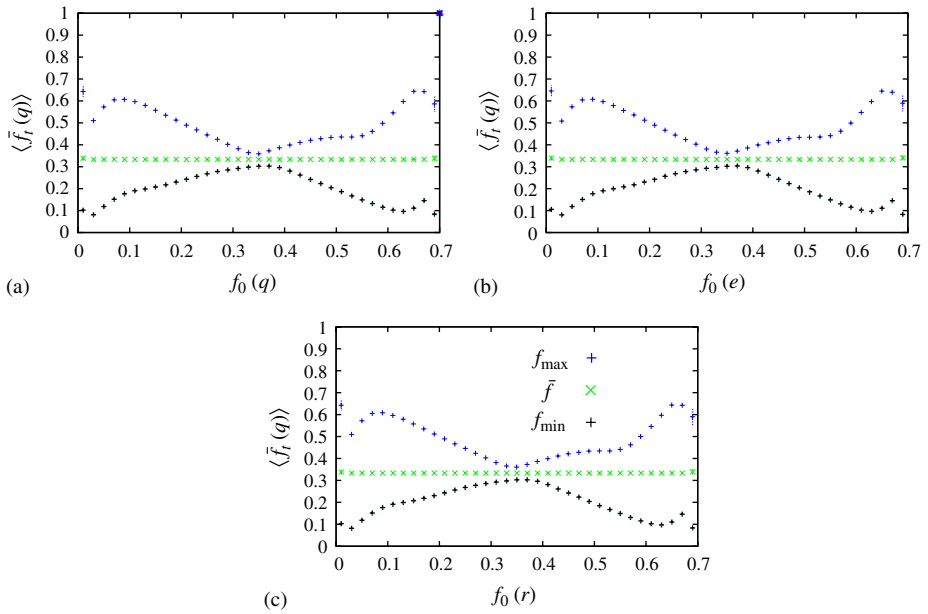

Fig. 4. Symmetry properties with respect to the macroscopic initial state $[f_0(e), f_0(q), f_0(r)]$. Identical plots are obtained displaying the minimal, maximal and average fractions of quiescent nodes in the periodic regime as a function, of $f_0(q)$ with $f_0(r) = 0.3$ (a), of $f_0(e)$ with $f_0(q) = 0.3$ (b), and of $f_0(r)$ with $f_0(e) = 0.3$ (c) (in all plots, we used 1000 instances of 10-Poisson networks). See the end of Section 2.8 for details on our notations.

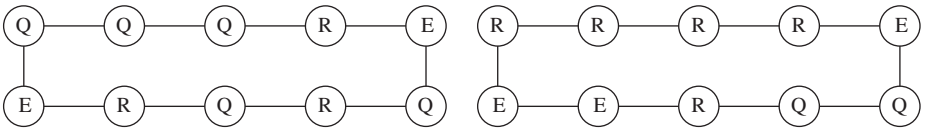

Fig. 5. A specially designed instance for which the generic identities pointed out in Fig. 4 should lead to the same fraction of quiescent nodes in the asymptotic regime if they were reflecting an exact symmetry of the dynamics.

These numerical experiments show that, for typical networks, notwithstanding their topology, the observed behaviors are very robust with respect to the initial state; the variability is larger in case of non-typical initial states. As already discussed, non-typical initial states (say, $f_0(e) < 0.03$ or $f_0(q) < 0.03$) on non-typical networks tend to give trivial asymptotic dynamics; this is confirmed here as all the nodes are eventually in the quiescent state.

Fig. 4 displays another feature of interest: that there exists symmetry relations between initial states, leading to exactly *identical* dynamic plots as shown here on typical Poisson networks; similar symmetry properties are observed with other average degrees and with power-law networks. It is important to notice that these symmetries are statistical by nature, and are *not* a mere consequence of the dynamics and the ensuing relation $f_{t+1}(r) = f_t(e)$. Indeed, Fig. 5 displays an instance designed especially to give a counter-example. The leftmost evolution starts from a $(0.5, 0.3, 0.2)$-initial state and the rightmost from a $(0.2, 0.5, 0.3)$-initial state; they should therefore lead to similar macroscopic states according to the symmetries depicted in Fig. 4. And yet, in the first case one obtains a steady macroscopic state where the fraction of nodes in each state are $f(q) = 0.6$, $f(r) = 0.2$, and $f(e) = 0.2$, while they are $f(q) = 0.8, f(r) = 0.1$, and $f(e) = 0.1$ in the second case. This counter-example reveals that we do not face a symmetry of the dynamics in all the cases but a statistical feature of the evolution and/or of the topology, as observed at the macroscopic level: the observed symmetries generically hold true but fail to be satisfied in some particular cases. One may wonder if there exists *typical* such instances, but this is out of the scope of this paper.

5. Convergence time

The results stated in Sections 3 and 4 involved fractions of nodes in each state, i.e., spatially averaged quantities, what is called ''order parameters'' in the language of statistical mechanics. Let us now turn to microscopic features, i.e., properties observed at the level of individual trajectories, in the phase space S^N. In the present section, we focus on the convergence time, namely the number of steps required to reach from a given initial condition the corresponding asymptotic periodic trajectory. We shall compare Poisson networks with power-law ones, for wide ranges of average degrees and exponents. In each case, we shall consider two initial states, one typical and the other one representative of what we termed non-typical initial states, i.e., with at least one very low fraction of nodes in one of the three states.

5.1. Poisson networks

The convergence time for Poisson networks is plotted in Figs. 6a–b as a function of the average degree (empirical average computed in each sample), with both typical initial conditions (Fig. 6a) and non-typical ones (Fig. 6b). This figure illustrates that the initial states and the topology play a somewhat similar role: whereas in typical cases the convergence time is very robust (almost constant), non-typical initial states or non-typical networks exhibit a stronger variability of the convergence time. Nevertheless, a remarkable fact is the small statistical dispersion here observed. For both non-typical networks and non-typical initial states, the convergence time is surprisingly less scattered than when only one of them is non-typical. This may be due to the fact that, in these cases, the effective network, i.e., the largest connected component of a random network of 1000 nodes, may actually be much smaller than the whole network thus finite-size effects take place (e.g. non-typical initial states may lead to a null number of initially excited nodes).

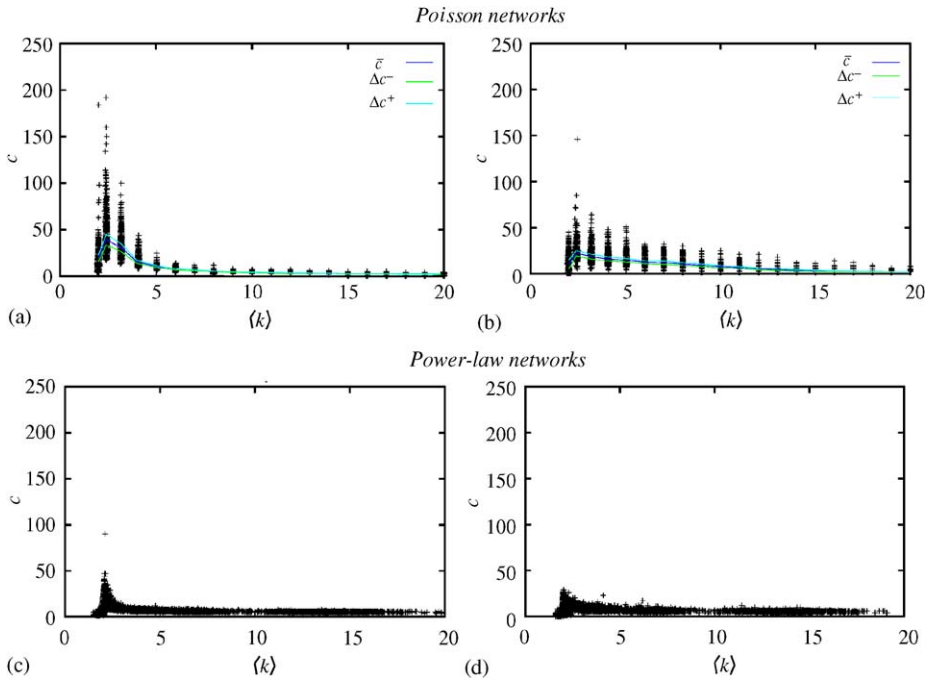

Fig. 6. Convergence time c as a function of the average degree for Poisson (a and b) and power-law networks (c and d). For k-Poisson networks, 1000 instances of networks are sampled for each integer value of k from 2 to 20. For power-law networks, 1000 instances of α-power-law networks are sampled for each value of the exponent α from 1.5 to 5 with step 0.25. In each case, their convergence time (starting from a typical initial state) is plotted (+). Moreover, the ensemble average $\bar{c}$ of the convergence time over each such sample, and its statistical dispersion, as visualized by $\bar{c}$, Δc^- and Δc^+ are plotted with lines. (a) With $(0.3, 0.3, 0.4)$-initial states for Poisson networks, (b) with $(0.69, 0.3, 0.01)$-initial states for Poisson networks, (c) with $(0.3, 0.3, 0.4)$-initial states for power-law networks and (d) with $(0.69, 0.3, 0.01)$-initial states for power-law networks.

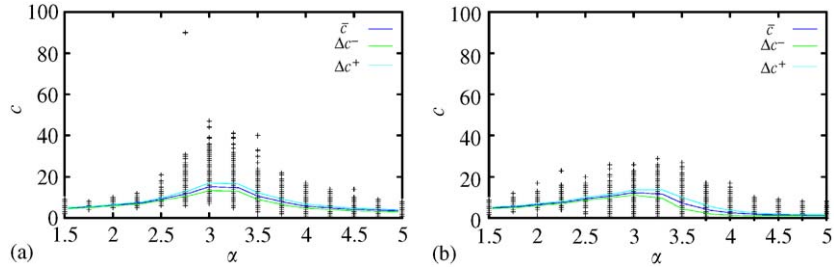

Fig. 7. Convergence time c as a function of the exponent α for power-law networks. For each value of α from 1.5 to 5 with step 0.25, 1000 instances of an α-power-law network and its initial state are sampled, and the associated convergence times are plotted. Moreover, the average $\bar{c}$ over each such sample, and Δc^- and Δc^+ are plotted with lines. (a) With typical $(0.3, 0.3, 0.4)$-initial states and (b) with non-typical $(0.69, 0.3, 0.01)$-initial states.

5.2. Power-law networks

We display in Figs. 6c–d similar plots for power-law networks. Despite they are obtained by varying the exponent α, which is the relevant control parameter for such networks, we present plots as a function of the average degrees (empirical average computed in each sample), and at the same scale as for Poisson networks (Figs. 6a–b), in order to make the comparison easier. We shall present and discuss the same results plotted as a function of the exponent below.

The general behavior is the same as for Poisson networks: the convergence time is very robust for typical networks and initial states, but varies significantly and may be very large with non-typical networks or non-typical initial states. However, it is clear from these plots that the convergence time is much less scattered on power-law than on Poisson networks. This may be viewed as a quantitative consequence of the fact, discussed in the preliminaries (Section 2), that the average distance in such networks is significantly lower than in Poisson networks; therefore, the dynamics runs faster, reflecting in a shorter convergence time.

The natural control parameter for power-law networks being the exponent α of the power-law degree distribution, let us now describe the influence of α on the convergence time (Fig. 7). The convergence time reaches its maximum value for exponents between 3 and 3.5, for which the average degree is close to 2. It also has its maximal variability for these exponent values, but remarkably, this variability remains moderate in all cases. Smaller exponents yield a result similar to Poisson networks with large average degrees: the convergence time is small and very robust. For larger values of the exponents, the convergence time remains short and not very scattered. This can be traced back to finite-size effects, since for $\alpha > 3.5$, the effective network, i.e., the connected component, is strongly reduced (typically smaller than 10% of the initial set of nodes). In the case of non-typical initial states, these finite-size effects are still stronger, since very few nodes, if any, are initially in the excited state, and so the dynamics is trivial. Like in the case of Poisson networks, the conclusion is that non-typical initial states increase the variability for typical networks, but decreases it for non-typical ones.

6. Period

Our aim is now to study the period p of the dynamics, along similar lines as those we followed for the convergence time (Section 5). Since the dynamics is deterministic, the system will *always* reach a periodic regime. But the number of possible states is huge (3^N) and this periodicity might a priori be irrelevant (undetectable) in a finite observation time. The striking result we shall present here is that it is not the case in typical situations: a finite, even small, period p is observed. This periodicity means that many initial conditions will evolve towards the same periodic trajectory. We plot this (microscopic) period p as a function of the average degree for Poisson networks in Figs. 8a–b, for power-law networks in Figs. 8c–d, and finally as a function of the exponent α of power-law networks in Fig. 9.

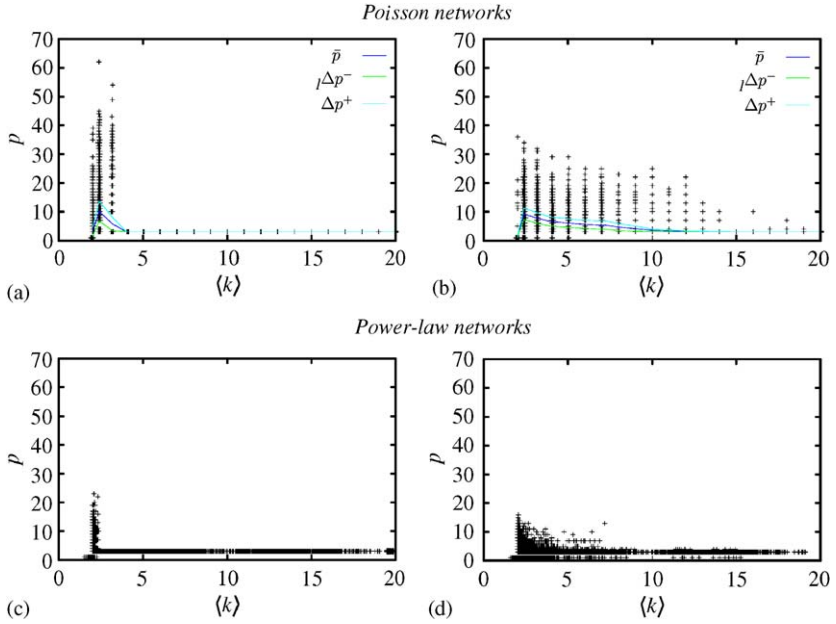

Fig. 8. Period p as a function of the average degree for Poisson (a and b) and power-law (c and d) networks. For each network category, 1000 instances are sampled (together with initial conditions). The observed period for each instance is plotted (+) for each integer value of k from 2 to 20, for k-Poisson network and for each value of the exponent α from 1.5 to 5 with step 0.25 for α-power-law networks. Moreover, the sample average $\bar{p}$ and Δp^- and Δp^+ are plotted with lines. (a) With typical $(0.3, 0.3, 0.4)$-initial states, (b) with non-typical $(0.69, 0.3, 0.01)$-initial states, (c) with typical $(0.3, 0.3, 0.4)$-initial states and (d) with non-typical $(0.69, 0.3, 0.01)$-initial states.

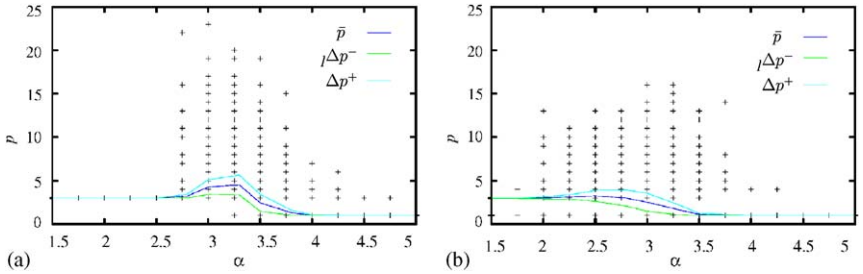

Fig. 9. Period as a function of the exponent for power-law networks. For each value of the exponent α from 1.5 to 5 with step 0.25, 1000 instances of a α-power-law networks and its initial state are sampled and the associated periods p are plotted. Moreover, the sample average $\bar{p}$ and $\bar{p}$ plus (resp. minus) the average difference between $\bar{p}$ and values larger (resp. smaller) than $\bar{p}$ are plotted with lines. (a) With typical $(0.3, 0.3, 0.4)$-initial states and (b) with non-typical $(0.69, 0.3, 0.01)$-initial states.

The results confirm what was observed for the convergence time. First, the period is very robust for typical networks and typical initial states. In other cases, quite different values may be obtained, but most of them are very close to the average. Taking non-typical initial states on typical networks and non-typical networks with typical initial states increases the variability. Finally, non-typical initial states on non-typical networks lead to less variability than these two last cases, due to the reduced size of the effective (connected) network underlying the dynamics.

These observations are valid on both Poisson and power-law networks, but again the results are less scattered for power-law networks than for Poisson ones. This can be viewed as a consequence of the existence of longer cycles (i.e., closed paths) in Poisson networks than in power-law ones.

Let us notice that the period often takes its minimal value $p = 3$. It indicates that no node remains in the same state several time steps in a row. In these cases, the macroscopic evolution may be described very easily

since $f_t(e) = f_{t-1}(q) = f_{t+1}(r)$. Notice, however, that this does not imply that these fractions are equal to $\frac{1}{3}$; only the time averages over a period are equal to $\frac{1}{3}$ (since $f_{t-1}(q) + f_t(q) + f_{t+1}(q) = 1$). At the microscopic level, each e becomes r, each r becomes q, hence necessarily each q becomes e. Hence in the asymptotic periodic regime with $p = 3$, the evolution reduces to synchronized flips $q \to e \to r \to q$ with no latency in state q. The excitable dynamics thus exhibits a kind of synchronization, but with a phase shift between neighbors, hence associated with a very complicated and heterogeneous spatial structure.

In case of non-typical networks, the fact that the asymptotic regime reduces to an equilibrium state where all the nodes are quiescent can be explained easily. Indeed, in such cases, as explained in the preliminaries (Section 2), the network is often a tree, and one can prove by a simple recursion that the dynamics vanishes in this case. Instead, as we have seen in Section 3, large cycles in the network may induce large periods and convergence times. Such cycles exist only in non-typical networks. These two points together explain the irregular behaviors observed for non-typical networks.

7. Conclusion and perspectives

In this contribution, we proposed a simple framework to study the dynamic behavior of coupled excitable units. Analytic approaches, relying on mean-field or pair-correlation approximations, are insufficient to faithfully capture the influence of network topology and initial state on phase-space trajectories. We thus conducted a wide set of simulations. We focused on both macroscopic features, namely the average, minimal, and maximal fractions of nodes in a given state in the periodic regime, and microscopic features, namely the period of the asymptotic regime and the convergence time, at the level of phase-space trajectories. Our investigations led us to introduce, as major determinants of the observed dynamic behavior, a notion of typical networks vs. non-typical ones (those of low average degree, close to 2) and a notion of typical initial states vs. non-typical ones (those with at least one very low fraction, say $f < 0.03$).

Our first conclusion is that the behavior is very robust on typical networks and with typical initial states: both the convergence time and the period are almost independent of the sample. When one turns to non-typical networks and non-typical initial states, the variability increases. This may be seen as a consequence of the fact that non-typical networks have large tree-like structures and cycles, which we have shown, play an important role in the dynamics: they make it possible to design topologies with arbitrarily large convergence time and period.

Our second conclusion is that the dynamics is more robust on power-law networks than on Poisson ones, which may basically be a consequence of the existence of shorter paths in power-law networks than in Poisson ones.

However, the behaviors of the dynamics on the two kinds of networks are quite similar: they do not vary qualitatively like in the cases of network tolerance to failures and attacks [18–23] or diffusion processes [14–17]. This leads us to our main conclusion: the dynamics studied here is only slightly sensitive to variations in the degree distribution of the underlying topology; instead, it is highly related to the presence (and number) of triangles and larger loops. It would therefore be highly relevant to now turn to studies addressing the influence of the number of triangles and loops in the underlying topology on the dynamics. It appears clearly from our study that this influence is central, and interesting behaviors would certainly be observed if we focus on this parameter.

Let us however note that such a study is challenging, since one would have to use models of topologies with triangles. The ones we used here, which are among the most classical ones in complex network studies, have a number of triangles which vanishes for large network sizes (though more slowly for power-law networks than for Poisson ones [7]). They have the advantage of uniformly sampling random graphs in a given class, and are widely accepted as reference models. On the contrary, there is currently no known method to sample *uniformly* a random graph with a given number of triangles. One would therefore have to use one of the many models proposed to generate specific networks with many triangles, see for instance [8,53]. But each such model has its own advantages and drawbacks, and there is currently no consensus on which model to use in experiments like the ones we conducted here. Although much progress has been done in this direction, there is still much to do.

Finally, we therefore consider the study of the influence of the number of triangles in the network as one of the most promising, but challenging, directions for further research.

There are of course many other directions which may be explored to extend our work. Let us begin with the precise study of size effects. We conducted experiments on networks with up to 100 000 nodes, and the results were similar in most cases, but some computations are intractable for such sizes. Also, modeling dynamics on directed and/or weighted networks remains to be done, but most of our framework and methodology can be extended straightforwardly to these cases. By contrast, the issue of pattern formation, ubiquitous in cellular automata studies, is here very complex since there is no simple underlying space. Finally, one may study the impact of variations in the dynamic rules: the refractory stage may last several time steps, one may associate an activation threshold to each node (thus prescribing the number of excited neighbors required to become excited), one may consider stochastic rules to model internal noise or external influences (such variants have been studied for SIS/SIR models), etc. An approach similar to the one presented here is relevant in all such instances.

Conversely, the influence of the topology on dynamics may be used to infer topological properties (which could not be directly measured) from the observed evolution. Such an inverse problem could be tackled successfully only if different topologies discriminate clear-cut dynamic features, which seems not to be the case for excitable dynamics (but the path has been traveled with some success for random Boolean networks [54]).

Finally, we would like to emphasize the fact that analytic approaches would be of high interest to describe dynamics of the kind we discussed here. Exact solutions seem presently unreachable but mean-field approximations and higher-order correlation equations may provide reference points with which to compare simulation results. However, using such approaches in this context remains a challenging task.

Acknowledgments

We thank anonymous referees for their helpful comments. This work was supported in part by the *Graphs, Algorithms and Probabilities* (GAP) project.

References

[1] K. Kohn, Molecular interaction map of the mammalian cell cycle control and DNA repair system, Mol. Biol. Cell 10 (1999) 2703–2734.
[2] P. Uetz, L. Giot, G. Cagney, T.A. Mansfield, R.S. Judson, J.R. Knight, D. Lockshon, V. Narayan, M. Srinivasan, P. Pochart, A. Qureshi-Emili, Y. Li, B. Godwin, D. Conover, T. Kalbfleisch, G. Vijayadamodar, M. Yang, M. Johnston, S. Fields, J.M. Rothberg, A comprehensive analysis of protein–protein interactions in *Saccharomyces cerevisiae*, Nature 403 (2000) 623–627.
[3] H. Jeong, B. Tombor, R. Albert, Z.N. Oltvai, A.L. Barabasi, The large-scale organization of metabolic networks, Nature 407 (2000) 651–654.
[4] I.J. Farkas, I. Derényi, H. Jeong, Z. Neda, Z.N. Oltvai, E. Ravasz, A. Schrubert, A.L. Barabasi, The topology of the transcription regulatory network in the yeast *Saccharomyces cerevisiae*, Physica A 318 (2003) 601–612.
[5] M.E.J. Newman, The structure of scientific collaboration networks, Proc. Nat. Acad. Sci. USA (2001) 404–409.
[6] R. Albert, A.-L. Barabási, Statistical mechanics of complex networks, Rev. Mod. Phys. 74 (2002) 47–97.
[7] M.E.J. Newman, The structure and function of complex networks, SIAM Rev. 45 (2003) 167–256.
[8] S.N. Dorogovtsev, J.F.F. Mendes, Evolution of networks, Adv. Phys. 51 (2002) 1079–1187.
[9] S.H. Strogatz, Exploring complex networks, Nature 410 (2001) 268–276.
[10] S.N. Dorogovtsev, J.F.F. Mendes, Evolution of Networks: From Biological Nets to the Internet and WWW, Oxford University Press, Oxford, 2000.
[11] S. Bornholdt, H.G. Schuster (Eds.), Handbook of Graphs and Networks: From the Genome to the Internet, Wiley-VCH, 2003.
[12] B. Bollobas, Random Graphs, Cambridge University Press, Cambridge, 2001.
[13] P. Erdös, A. Rényi, On random graphs I, Publ. Math. Debrecen 6 (1959) 290–297.
[14] M. Barthélémy, A. Barrat, R. Pastor-Satorras, A. Vespignani, Dynamical patterns of epidemic outbreaks in complex heterogeneous networks, J. Theoret. Biol. 235 (2005) 275–288.
[15] R. Pastor-Satorras, A. Vespignani, Epidemic spreading in scale-free networks, Phys. Rev. Lett. 86 (2001) 3200–3203.
[16] M.E.J. Newman, The spread of epidemic disease on networks, Phys. Rev. E 66 (2002) 016128.
[17] Z. Dezsö, A.-L. Barabási, Halting viruses in scale-free networks, Phys. Rev. E 65 (2002) 055103.
[18] R. Albert, H. Jeong, A.-L. Barabási, Error and attack tolerance in complex networks, Nature 406 (2000) 378–382.
[19] R. Cohen, K. Erez, D. Ben-Avraham, S. Havlin, Resilience of the internet to random breakdown, Phys. Rev. Lett. 85 (2000) 4626–4629.
[20] R. Cohen, K. Erez, D. Ben-Avraham, S. Havlin, Breakdown of the internet under intentional attack, Phys. Rev. Lett. 86 (2001) 3682–3685.

[21] D.S. Callaway, M.E.J. Newman, S.H. Strogatz, D.J. Watts, Network robustness and fragility: percolation on random graphs, Phys. Rev. Lett. 85 (2000) 5468–5471.
[22] A.E. Motter, Y.-C. Lai, Cascade-based attacks on complex networks, Phys. Rev. E 66 (2002) 046139.
[23] S. Nikoletseas, G. Prasinos, P.G. Spirakis, C.D. Zaroliagis, Attack propagation in networks, in: ACM Symposium on Parallel Algorithms and Architectures, 2001, pp. 67–76.
[24] K. Kaneko, I. Tsuda, Complex Systems: Chaos and Beyond, Springer, Berlin, 2000.
[25] S. Wolfram, Statistical mechanics of cellular automata, Rev. Mod. Phys. 55 (1983) 601–644.
[26] S. Wolfram, Universality and complexity in cellular automata, Physica D 10 (1984) 1–35.
[27] G.B. Ermentrout, L. Edelstein-Keshet, Cellular automata approaches to biological modelling, J. Theoret. Biol. 160 (1993) 97–133.
[28] B. Chopard, M. Droz, Cellular Automata Modeling of Physical Systems, Cambridge University Press, Cambridge, 1998.
[29] D. Watts, S. Strogatz, Collective dynamics of small-world networks, Nature 393 (1998) 440–442.
[30] C. Marr, M.T. Hütt, Topology regulates pattern formation capacity of binary cellular automata on graphs, Physica A (2005).
[31] J.F. Fox, C.H. Hill, From topology to dynamics in biochemical networks, Chaos (2001).
[32] M. Aldana, Boolean dynamics with scale-free topology, Physica D 185 (2003) 45–66.
[33] S.A. Kauffman, Metabolic stability and epigenesis in randomly constructed nets, J. Theoret. Biol. 22 (1969) 437–467.
[34] S.A. Kauffman, The large scale structure and dynamics of gene control circuits: an ensemble approach, J. Theoret. Biol. 44 (1974) 167–190.
[35] E. Lieberman, C. Hauert, M.A. Nowak, Evolutionary dynamics on graphs, Nature 433 (2005) 312–316.
[36] J.J. Hopfield, Neural networks and physical systems with emergent collective computational abilities, Proc. Nat. Acad. Sci. USA 79 (1982) 2554–2558.
[37] G.K. Moe, W.C. Rheinboldt, J.A. Abildskov, A computer model of atrial fibrillation, Am. Heart J. 67 (1964) 200–220.
[38] C. Meunier, D. Hansel, A.D. Verga, Information processing in three-state neural networks, J. Statist. Phys. 55 (1989) 859–901.
[39] D.R. Carreta Dominguez, E. Korutcheva, Three-state neural network: from mutual information to the hamiltonian, Phys. Rev. E 62 (2000) 2620–2628.
[40] C. Meunier, H.F. Yanai, S. Amari, Sparsely coded associative memories: capacity and dynamical properties, Network 2 (1991) 469–487.
[41] T.I. Netoff, R. Clewey, S. Arno, T. Keck, J.A. White, Epilepsy in small-world networks, J. Neurosci. 24 (2004) 8075–8083.
[42] C.C. Hilgetag, M. Kaiser, Clustered organization of cortical connectivity, Neuroinformatics 2 (2004) 353–360.
[43] O. Sporns, G. Tononi, G.M. Edelman, Connectivity and complexity: the relationship between neuroanatomy and brain dynamics, Neural Networks 13 (2000) 909–922.
[44] O. Diekmann, J. Heesterbeek, Mathematical Epidemiology of Infectious Diseases: Model Building, Analysis and Interpretation, Wiley, New York, 2000.
[45] J.O. Kephart, S.R. White, Directed-graph epidemiological models of computer viruses, in: Proceedings of the IEEE Computer Society Symposium on Research in Security and Privacy, 1991, pp. 343–359.
[46] G. Abramson, M. Kuperman, Small world effect in an epidemiological model, Phys. Rev. Lett. 86 (2001) 2909–2912.
[47] D.H. Zanette, Critical behavior of propagation on small-world networks, Phys. Rev. E 64 (2001) 050901.
[48] J.-L. Guillaume, Random network generators, http://www.liafa.jussieu.fr/~guillaume/index.php?page=programs
[49] M. Molloy, B. Reed, A critical point for random graphs with a given degree sequence, Random Struct. Algorithms 6 (1995) 161–180.
[50] A.-L. Barabási, R. Albert, Emergence of scaling in random networks, Science 286 (1999) 509–512.
[51] F. Viger, M. Latapy, Random generation of large connected simple graphs with prescribed degree distribution, in: Lecture Notes in Computer Science (LNCS) 3595, Proceedings of the 11th International Conference on Computing and Combinatorics COCOON 2005, Kunming, China, 2005, pp. 440–449.
[52] M. Molloy, B. Reed, The size of the giant component of a random graph with a given degree sequence, Combin. Probab. Comput. 7 (1998) 295–306.
[53] J.-L. Guillaume, M. Latapy, Bipartite graphs as models of complex networks, in: Lecture Notes in Computer Sciences (LNCS), Proceedings of the First International Workshop on Combinatorial and Algorithmic Aspects of Networking (CAAN), 2004.
[54] S. Kim, J.N. Weinstein, J.J. Grefenstette, Inference of large-scale topology of gene regulation networks by neural nets, in: Proceedings of the IEEE International Conference of Systems, Man, and Cybernetics, 2003, pp. 3969–3975.